Supplementary information for:

Immunostimulatory effects of targeted thorium-227 conjugates as single agent and in combination with anti-PD-L1 therapy

Pascale Lejeune[1], Véronique Cruciani[2], Axel Berg-Larsen[2], Andreas Schlicker[1], Anne Mobergslien[2], Lisa Bartnitzky[1], Sandra Berndt[1], Sabine Zitzmann-Kolbe[1], Claudia Kamfenkel[1], Stefan Stargard[1], Stefanie Hammer[1], Jennifer S Jørgensen[3], Malene Jackerott[3], Carsten H Nielsen[3], Christoph A Schatz[1], Hartwig Hennekes[1], Jenny Karlsson[2], Alan S Cuthbertson[2], Dominik Mumberg[1] and Urs B Hagemann[1]

[1]Bayer AG, Pharmaceuticals Division, Berlin, Germany; [2]Bayer AS, Oslo, Norway; [3]Minerva Imaging ApS, Copenhagen, Denmark

SUPPLEMENTARY METHODS

Quantitative RT-PCR and RNASeq analysis

Upregulation of mRNA levels was analyzed from tumor samples by TaqMan-based RT-qPCR. The following murine probes were used: Ifnb1 (Mm00439552_s1), Mx1(Mm00487796_m1), Ifnar1 (Mm00439544_m1), Tmem173 (Mm01158117_m1), Cxcl10 (Mm00445235_m1), GAPDH (Mm99999915_g1), Ncr1 (Mm01337324_g1), Cd274 (Mm00452054_m1), Foxp3 (Mm00475162_m1), TNF (alpha) (Mm00443258_m1), IL-2 (Mm00434256_m1), IL-6 (Mm00446190_m1), IFNg (Mm01168134_m1), IL-10 (Mm00439614_m1), Tgfb1 (Mm01178820_m1), Mrc1/CD206 (Mm00485148_m1), Prf1 (Mm00812512_m1). All probes were purchased from Applied Biosystems.

In parallel, supernatant collected from treated cells (n = 2 samples/treatment) as well as tumor tissue and lymph node lysates (n = 3 animals/group) were analyzed for inflammatory cytokines using customized 10-U-PLEX plates (Meso Scale Discovery).

For RNASeq analysis, MC38-hMSLN and OVCAR-3 cells were treated in triplicate for 72 hours with vehicle, non-radiolabeled MSLN-antibody chelator conjugate, or MSLN-TTC (0.5, 5, and 50 kBq/kg). RNA was isolated with the Qiagen RNA isolation kit according to the manufacturer's protocol. RNA sequencing was performed at Eurofins Genomics. Poly-A-enriched mRNA was sequenced using 50 bp single-end reads. RNASeq reads were aligned using STAR aligner to Gencode GRCm38, version M16, for MC38 and to Gencode GRCh38, version 28, for OVCAR-3. Gene expression was quantified using RSEM, version 1.3.0. Differential gene expression analysis was performed using DESeq2, version 1.26.0 (1). Genes were considered to be differentially expressed compared to vehicle treatment if the absolute log2 fold change

was greater than 2 and the false discovery rate less than 0.05.

Gene Set Enrichment Analysis was performed using the fgsea package for R, version 1.10.1 (2), with log2 fold changes as input. Gene sets were taken from the Molecular Signatures Database v7.1 (3) including Hallmark gene sets (4) and KEGG pathways (5). Mouse genes were mapped to their human ortholog obtained from Ensembl, version 101 (6). This mapping was also used to convert gene identifiers in pathway lists to mouse genes.

Analysis of DAMP and immunomodulatory marker expression by flow cytometry

Cells were cultured in RPMI (Biowest) supplemented with 10% fetal bovine serum (Hyclone), non-essential amino acids (Gibco), sodium pyruvate (Gibco), penicillin/streptomycin (Biowest) and 0.5 µg/mL blasticidin (Thermo Fisher). The cells were seeded in six-well plates at a density of 1 x 10^5 cells/well and after a 24-h incubation exposed to MSLN-TTC or radiolabeled isotype control (specific activity of 40 kBq/µg; dose range 0.5–50 kBq/mL). After a 24- or 72-h exposure, the cells were harvested with Accutase (Biowest) and incubated with antibodies specific for the DAMPs: Alexa Fluor 647-conjugated calreticulin polyclonal antibody (Bioss Antibodies), Alexa Fluor 647-conjugated HSP70(Tyr41) polyclonal antibody (Bioss Antibodies), Alexa Fluor 647-conjugated GRP94 polyclonal antibody (HSP90 beta member 1, Bioss Antibodies), and Alexa Fluor 647-conjugated HMGB1 polyclonal antibody (Bioss Antibodies) on ice for 1 h.

Staining for immune response markers was performed using the following antibody panel: APC anti-mouse IFNAR-1 (Biolegend), APC anti-mouse CD252 (OX40L) (Biolegend), APC anti-mouse CD54 (Biolegend), APC anti-mouse CD152 (Biolegend),

APC anti-mouse CD274 (B7-H1, PD-L1, Biolegend), APC anti-mouse CD137 (Biolegend), Mouse CEACAM-1/CD66a APC-conjugated antibody (R&D Systems), Mouse B7-H2 Alexa Fluor 647-conjugated antibody (R&D Systems), Alexa Fluor 647-conjugated TRAILR1/TNFRSF10A antibody (32A242, Novus Biologicals), and Alexa Fluor 647-conjugated CD27 ligand/TNFSF7/CD70 antibody (TAN 1-7, Novus Biologicals). The flow cytometry analysis of living cells was performed in the presence of propidium iodide (Calbiochem).

Cells were fixed and permeabilized with cold 70% ethanol in parallel, followed by cell cycle analysis (FxCycle PI/RNase staining solution, Thermo Fisher), determination of the proportion of cells harboring DNA DSBs using Alexa Fluor 647-conjugated phospho-histone H2A.X (Ser139) (20E3) rabbit mAb (Cell Signaling Technology), and evaluation of the proportion of cells undergoing apoptosis as determined by the binding of Alexa Fluor 488-conjugated cleaved caspase-3 (Asp175) antibody (Cell Signaling Technology).

To analyze phosphorylation of STING after a 24, 48, 72, or 96-h exposure to MSLN-TTC, cells were fixed with 4% paraformaldehyde in phosphate-buffered saline (PBS), permeabilized with 0.2% Triton X-100 in PBS and stained with phospho-STING (S365) (D1C4T) Rabbit mAb (Cell Signaling Technology) detected with Alexa Fluor 647-conjugated donkey anti-rabbit IgG (minimal cross-reactivity, Biolegend).

All stainings were detected with Guava EasyCyte 8HT flow cytometer and the data analysis was performed using FlowJo software, version 10, and GraphPad Prism software, version 8.

Induction of immunogenic cell death was performed on human mononuclear cells, isolated from buffy coats through density gradient centrifugation using Lymphoprep

(Axis Shield) and followed by negative sorting of monocytes using magnetic beads (Miltenyi). Cells were cultured in RPMI (GIBCO) containing 100 ng/mL GM-CSF (R&D Systems), 20 ng/mL IL-4 (R&D Systems), 10% fetal bovine serum (FBS), and penicillin/streptomycin for 6 days. Immature dendritic cells were activated using media from OVCAR-3 cells exposed to MSLN-TTC (10 kBq/mL) *in vitro* for 5 days. Two-hundred µL of the cell supernatant was transferred to 100 µL of dendritic cell culture (100,000 cells/well) and incubated for 48 h. Cell maturation was analyzed with Guava easyCyte 8HT flow cytometer using fluorescent antibodies anti-CCR7-FITC (Miltenyi), anti-HLA-DR (Miltenyi), anti-DQ (Miltenyi), and anti-DL-APC (Miltenyi) and anti-86-PE (BioLegend).

Flow cytometry analysis on isolated tumors and tumor draining lymph nodes after treatment

The isolated tumors were cut into pieces and enzymatically digested (Tumor Dissociation kit, Miltenyi Biotec). The samples were placed in a 37°C water bath with shaking for 40 min. Both TdLNs and enzymatically digested tumor samples were passed through 70 µm cell strainers and diluted in PBS. The number of cells in each tumor sample was determined by using NucleoCounter® NC-202™ (Chemometec) according to the manufacturer's protocol. TdLN samples were pooled (two TdLNs per sample). All TdLN cells and approximately 10^6 cells from each tumor sample were Fc-blocked for 5 min (Purified Rat Anti-Mouse CD16/CD32, BD Biosciences) and surface-stained using a panel of antibodies (BUV395 Rat Anti-Mouse CD45, BUV496 Rat Anti-CD11b, BUV737 Hamster Anti-Mouse CD11c, BV605 Rat Anti-Mouse CD103, BV711 Rat Anti-Mouse F4/80, BV786 Rat Anti-Mouse CD8a, FITC Rat Anti-Mouse CD4 (BD Biosciences); Brilliant Violet 421™ anti-mouse CD206 (MMR) Antibody, PE anti-

mouse CD3ε Antibody, PE/Cyanine7 anti-mouse IFNAR-1 Antibody, APC anti-mouse I-A/I-E Antibody (BioLegend); Fixable Viability Dye eFluor™ 780 (eBioscience)). Tumor and TdLN samples were analyzed on a LSRFortessa X20 Flow Cytometer (BD Biosciences) with FlowJo 10.4 software (Treestar). Debris and doublets were excluded on the basis of forward and side scatter. Fluorescence minus one samples were included and used for correct identification of positive and negative cell populations.

Detection of secreted chemokines and cytokines using mesoscale technology

Secreted chemokines and cytokines were detected using mesoscale technology (Meso Scale Discovery). *In vitro*, OVCAR-3, OVCAR-8, or MC38-hMSLN cells were exposed for 120 h to either MSLN-TTC (0.5, 5, or 50 kBq/mL) or non-radiolabeled MSLN-antibody chelator conjugate or cGAMP (20 µg/mL). Cell supernatants were collected subsequently. Samples were processed with human and murine U-Plex customized kits (Meso Scale Discovery) according to the manufacturers' instructions.

Tumors from *in vivo* efficacy studies were isolated nine days after treatment and processed with the murine proinflammatory I and customized U-Plex kits (Meso Scale Discovery) according to the manufacturers' instructions. The amount of detected chemokines/cytokines were calculated using respective standard curves, supplied with each kit, and converted into x-fold changes in comparison to vehicle-treated animals.

SUPPLEMENTARY TABLES

Supplementary Table S1. *In vivo* efficacy of MSLN-TTC monotherapy.

Treatment	%T/C (on day 19)	Median time for tumor size to reach 300 mm^3 (days)	Median tumor growth delay (days)	Complete responders
Vehicle	(100)	13	-	0/11
MSLN-TTC 125 kBq/kg	32***	17	4	1/11
MSLN-TTC 250 kBq/kg	7***	40***	27***	3/11
MSLN-TTC 500 kBq/kg	5***	>121****	>108****	6/11

Mean comparisons of tumor volumes between the treatment and control groups were performed using the estimated linear model and corrected for family-wise error rate using Sidak's method. Statistical analysis on time to median tumor size 300 mm^3 or tumor growth delay was performed using Kruskal-Wallis and Dunn's tests. ***, $p < 0.001$, ****, $p < 0.0005$.

Supplementary Table S2. Effect of depletion of CD8 T-cells on T/C ratio and tumor doubling times volume in MSLN-TTC, anti-PD-L1, and MSLN-TTC/anti-PD-L1-treated, MC38-hMSLN tumor-bearing mice. Tumor volume ratios were calculated on day 20.

Treatment group	Treatment/control ratio on day 20		Tumor doubling time (days)	
	Non-CD8 depleted	CD8-depleted	Non-CD8 depleted	CD8-depleted
Vehicle	-		4.9	4.4
MSLN-TTC (250 kBq/kg)	0.23**	0.73***	11.5	4.5
Anti-PD-L1 (1.5 mg/kg)	0.31**	1.46	3.8	4.7
MSLN-TTC (250 kBq/kg) + anti-PD-L1 (1.5 mg/kg)	0.13***	0.45***, †,‡‡‡	51.6 **	5.3 †, ‡

Statistical analysis on tumor volumes was performed using a linear model estimated using generalized least squares and group comparisons were corrected for false positive rate using Sidak's method.

Statistical analysis on tumor doubling times was performed using Cox's proportional hazards regression model.

**, $p<0.01$; ***, $p<0.001$ compared to vehicle. †, $p<0.05$ compared to corresponding MSLN-TTC monotherapy. ‡, $p<0.05$; ‡‡‡, $p<0.001$ compared to corresponding anti-PD-L1 monotherapy.

Supplementary Table S3. Fold changes in *in vivo* expression of cytokines and chemokines in isolated MC38-hMSLN tumors. The protein level analysis was performed using Meso Scale Discovery nine days after treatment start and values are shown in comparison to vehicle.

	Cytokine														
Treatment	**CXCL10**	**CCL20**	**CCL3**	**CCL4**	**CCL2**	**IFN-β**	**IFN-γ**	**IL-6**	**IL-10**	**IL-1β**	**IL-2**	**IL-4**	**IL-5**	**IL12-p70**	**Kc/Gro**
MSLN-TTC (250 kBq/kg)	1.1	1.7	1.1	0.9	1.1	1.1	3.5	1.5	1.8	0.5	1.7	1.9	6.1	1.1	3.7
Anti-PD-L1 (1.5 mg/kg)	1.0	1.0	1.1	1.7	1.0	1.2	4.7	0.9	1.6	0.9	2.3	12.0	17.6	1.0	2.5
MSLN-TTC (250 kBq/kg) + anti-PD-L1 (1.5 mg/kg)	1.0	2.7	1.1	2.0	1.1	1.2	6.5	1.4	2.6	0.5	2.6	4.4	21.1	1.5	4.1

SUPPLEMENTARY FIGURES

Supplementary Figure 1

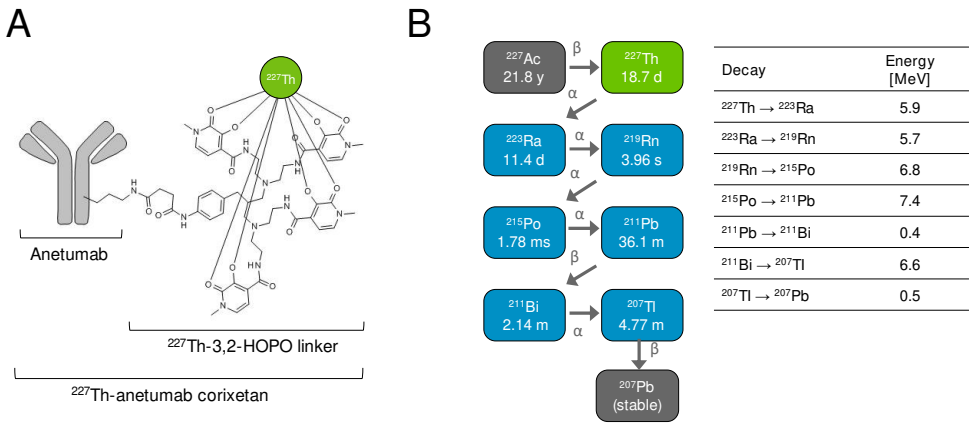

Decay	Energy [MeV]
$^{227}Th \rightarrow {}^{223}Ra$	5.9
$^{223}Ra \rightarrow {}^{219}Rn$	5.7
$^{219}Rn \rightarrow {}^{215}Po$	6.8
$^{215}Po \rightarrow {}^{211}Pb$	7.4
$^{211}Pb \rightarrow {}^{211}Bi$	0.4
$^{211}Bi \rightarrow {}^{207}Tl$	6.6
$^{207}Tl \rightarrow {}^{207}Pb$	0.5

Supplementary Figure S1.

A. Structure of MSLN-TTC (thorium (^{227}Th) anetumab corixetan) including the N-hydroxysuccinimide-activated 3,2-hydroxypyridinone (HOPO) chelator conjugated to anetumab.

B. Thorium-227 decay scheme. Thorium-227, $t_{1/2}$ = 18.7 days, is purified from an actinium-227 generator and it decays via its alpha and beta-emitting daughters to stable non-radioactive ^{207}Pb. ^{223}Ra will detach from the antibody-chelator conjugate due to the substantial kinetic energy of the recoiling nucleus after alpha particle emission.

Supplementary Figure S2

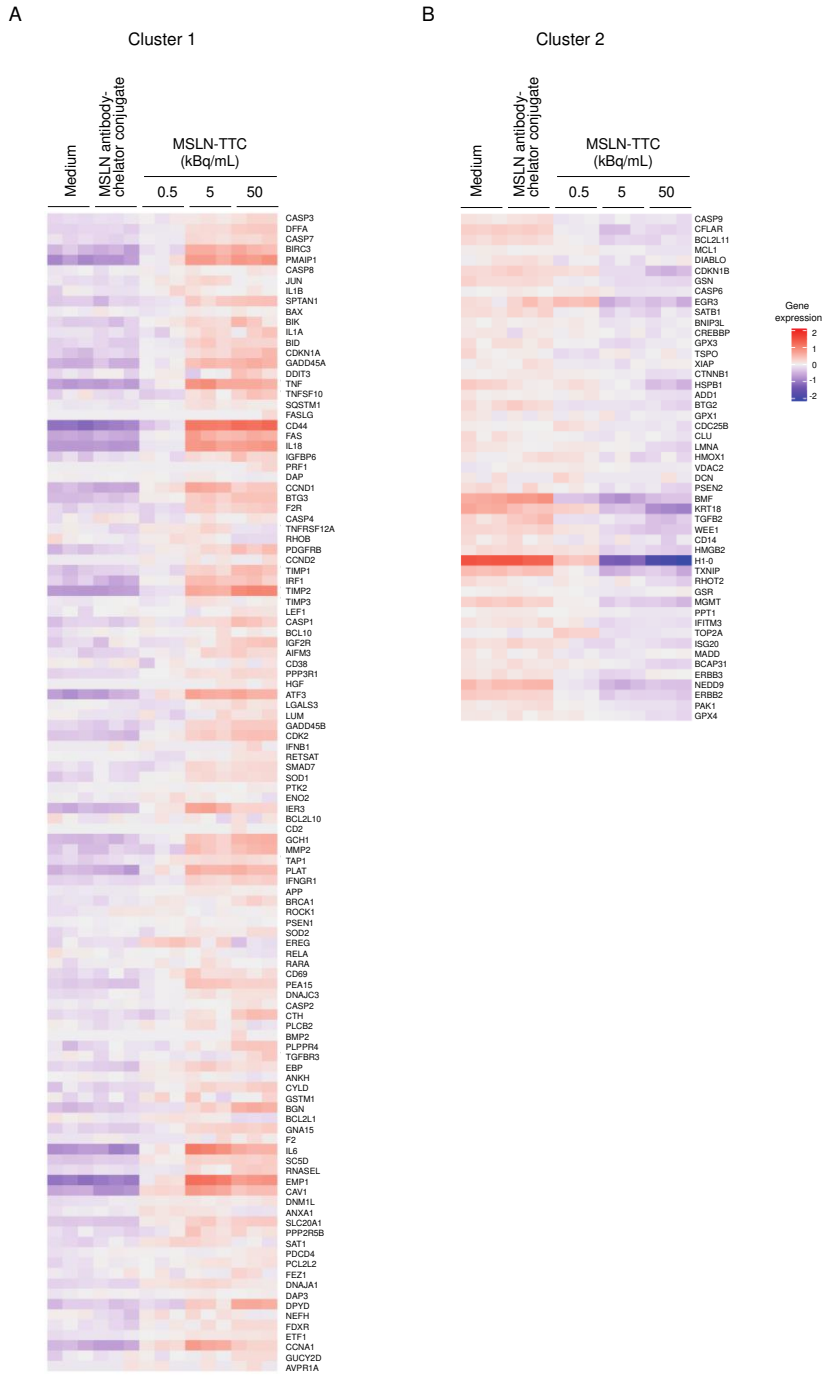

Supplementary Figure S2. Heatmap of deregulated hallmark apoptosis genes in human ovarian cancer OVCAR-3 cells upon exposure to MSLN-TTC after 72 h displaying log2 experssion values mean-centered by gene. (A) Cluster 1 and (B) Cluster 2.

Supplementary Figure S3

Supplementary Figure S3. Heatmap of deregulated hallmark apoptosis genes in MC38-hMSLN cells upon exposure to MSLN-TTC after 72 h displaying log2 expression values mean-centered by gene. (A) Cluster 1 and (B) Cluster 2.

Supplementary Figure S4

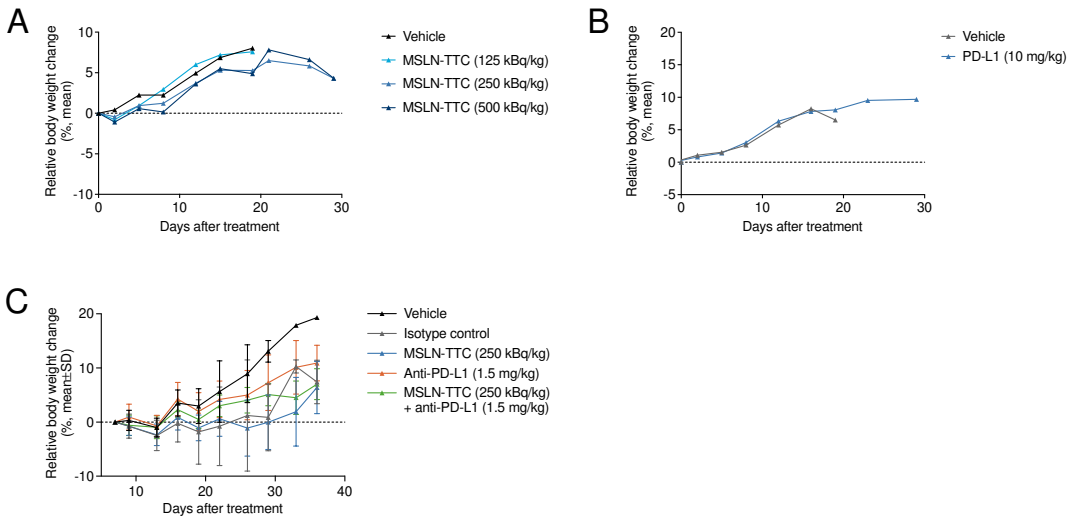

Supplementary Figure S4. Tolerability of MSLN-TTC and anti-PD-L1 therapies in immunocompetent MC38-hMSLN tumor-bearing mice.

A. Relative body weight change of mice during treatment after single-dose administration of MSLN-TTC at radioactivity doses of 125, 250 or 500 kBq/kg (i.v.).

B. Relative body weight change of mice during treatment after anti-PD-L1 treatment (10 mg/kg, Q3D, i.p.).

C. Relative body weight change of mice during treatment after administration of MSLN-TTC (a single dose, 250 kBq/kg, i.v.), anti-PD-L1 (1.5 mg/kg, Q3/4D, i.p.) and their combination.

Supplementary Figure S5

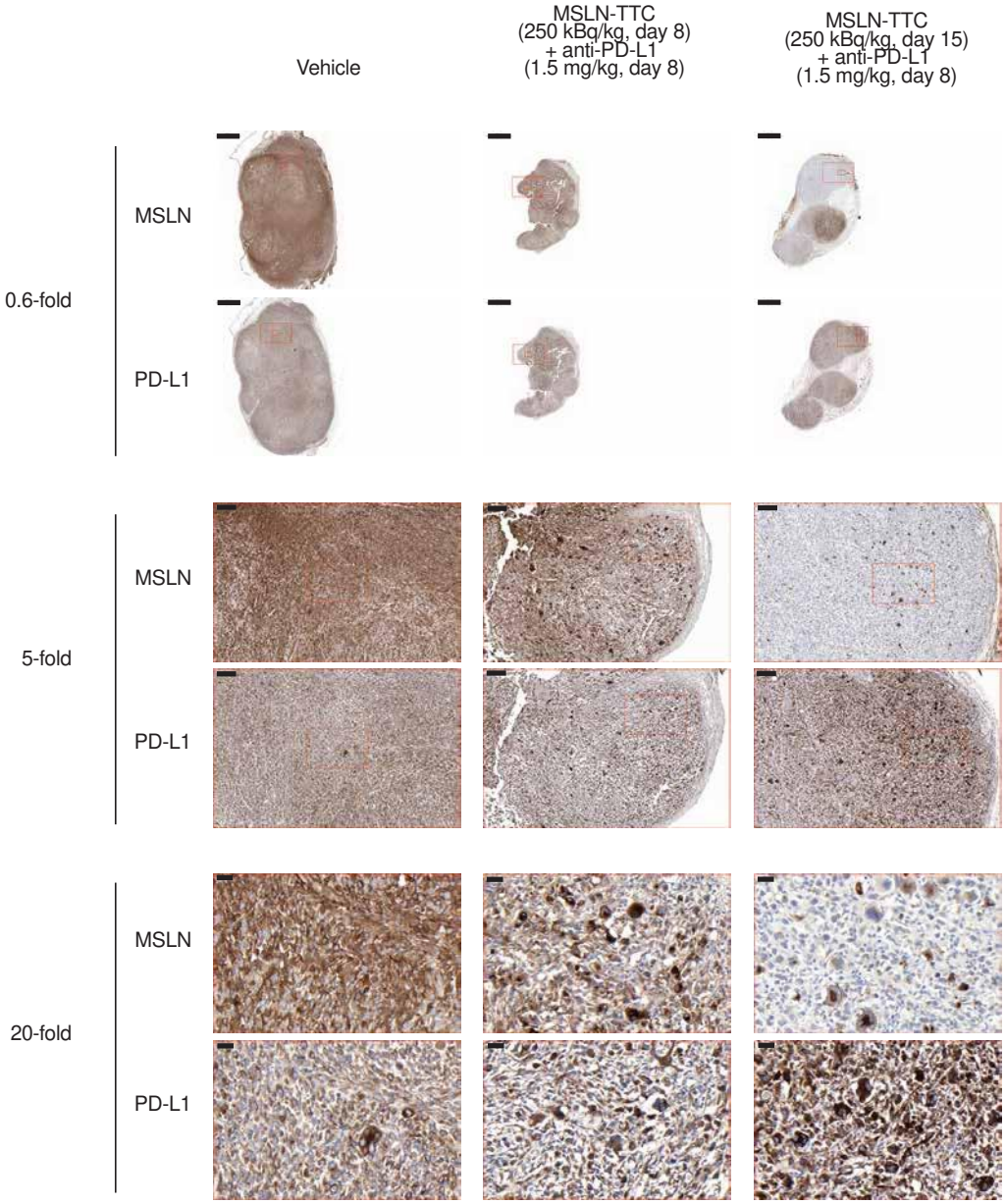

Supplementary Figure S5. MSLN and PD-L1 expression in MC38-hMSLN tumors in the dose-sequencing study as determined by IHC. Tumors were treated with vehicle, simultaneous administration of MSLN-TTC (250 kBq/kg) and anti-PD-L1 (1.5 mg/kg) on day 8, or sequential administration of anti-PD-L1 (1.5 mg/kg) on day 8,

followed by MSLN-TTC (250 kBq/kg) on day 15. Scale bars 1000 μm for 0.6-fold, 100 μm for 5-fold, and 20 μm for 20-fold magnifications, respectively.

Supplementary Figure S6

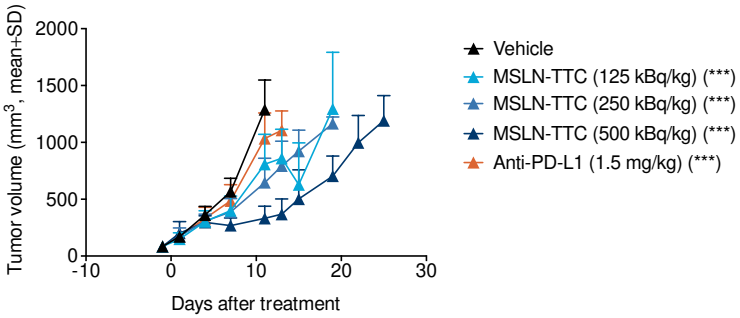

Supplementary Figure S6. *In vivo* efficacy of MSLN-TTC in fully immunocompromised Rag2/Il2rg knock-out mice treated with MSLN-TTC or anti-PD-L1 as indicated in the figure (n=12/group). Statistical analysis was performed using a linear model estimated with generalized least squares with a separate variance term for each group. Pairwise comparisons were performed using the estimated linear model and corrected for family-wise error rate using Dunnett's method. ***, $p<0.001$ compared to vehicle.

Supplementary Figure S7

A

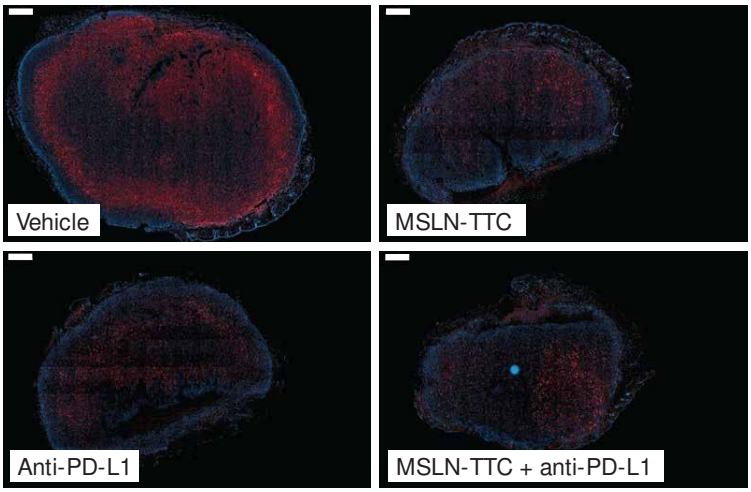

B

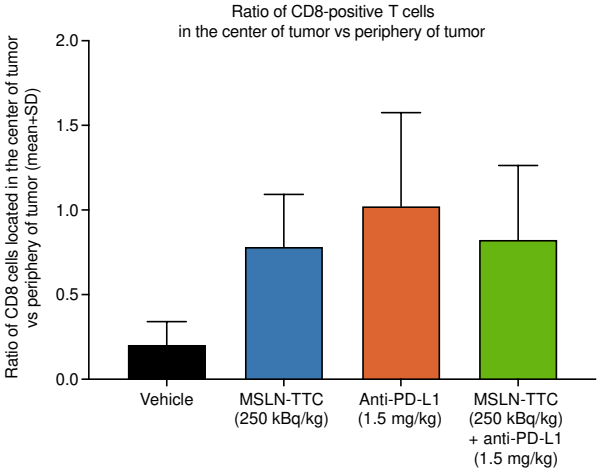

Supplementary Figure S7. **Analysis of CD8 T-cells in MC38-hMSLN tumors by IHC.** MSLN-TTC was administered at 250 kBq/kg (a single i.v. dose) and anti-PD-L1 at 1.5 mg/kg (Q3/4D, i.p.). Tumors were isolated 7 days after first treatment.

A. CD8 T-cells in tumors as detected by immunofluorescence imaging using rat anti-mouse CD8 mAb. Blue denotes DAPI staining of the nuclei and red denotes CD8

positive cells. Scale bars 500 µm.

B. Ratio of CD8 T-cells in the center of the tumor vs. in the periphery of the tumor (n = 3 mice/group) as determined by IHC quantification.

Supplementary Figure S8

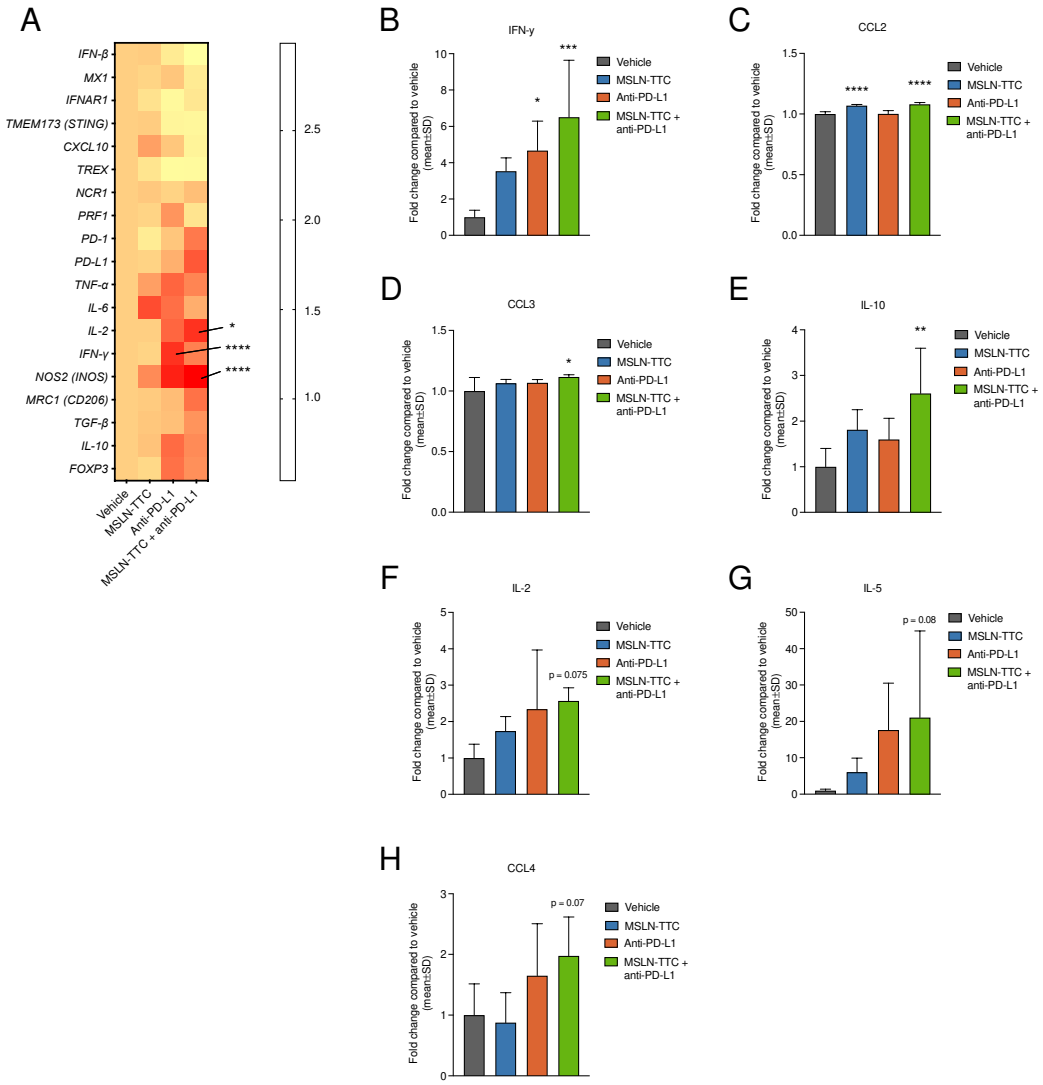

Supplementary Figure S8. **Gene transcripts and cytokine levels in MC38-hMSLN tumor samples after MSLN-TTC and anti-PD-L1 treatment.** MSLN-TTC was administered at 250 kBq/kg (a single i.v. dose) and anti-PD-L1 at 10 mg/kg (Q3/4D, i.p.).

A. Gene transcript levels in tumors (n = 3/group) as determined by TaqMan RT-qPCR five days after treatment. Values were normalized to *GAPDH* transcripts and are expressed as fold changes compared to vehicle-treated mice. Statistical analysis was performed using one-way ANOVA.

B.-I. Levels of cytokines (B) IFN-γ, (C) CCL2, (D) CCL3, (E) IL-10, (F) IL-2, (G) IL-5

and (H) CCL4 in tumors as determined by Meso Scale Discovery analysis nine days after treatment. Statistical analysis was performed using one-way ANOVA. *, $p<0.05$; **, $p<0.01$; ***, $p<0.001$; ****, $p<0.0001$ compared to vehicle.

References for Supplementary Materials

1. Love MI, Huber W, Anders S. Moderated estimation of fold change and dispersion for RNA-seq data with DESeq2. Genome Biol. 2014;15(12):550.

2. Korotkevich G, Sukhov V, Sergushichev A. Fast gene set enrichment analysis. bioRxiv. 2019.

3. Subramanian A, Tamayo P, Mootha VK, Mukherjee S, Ebert BL, Gillette MA, et al. Gene set enrichment analysis: a knowledge-based approach for interpreting genome-wide expression profiles. Proc Natl Acad Sci U S A. 2005;102(43):15545-50.

4. Liberzon A, Birger C, Thorvaldsdottir H, Ghandi M, Mesirov JP, Tamayo P. The Molecular Signatures Database (MSigDB) hallmark gene set collection. Cell Syst. 2015;1(6):417-25.

5. Kanehisa M, Furumichi M, Tanabe M, Sato Y, Morishima K. KEGG: new perspectives on genomes, pathways, diseases and drugs. Nucleic Acids Res. 2017;45(D1):D353-D61.

6. Zerbino DR, Achuthan P, Akanni W, Amode MR, Barrell D, Bhai J, et al. Ensembl 2018. Nucleic Acids Res. 2018;46(D1):D754-D61.

7. Vanpouille-Box C, Alard A, Aryankalayil MJ, Sarfraz Y, Diamond JM, Schneider RJ, et al. DNA exonuclease Trex1 regulates radiotherapy-induced tumour immunogenicity. Nat Commun. 2017;8:15618.